HHS Public Access

Author manuscript

ACS Appl Mater Interfaces. Author manuscript; available in PMC 2020 May 08.

Published in final edited form as:

ACS Appl Mater Interfaces. 2019 May 08; 11(18): 16402–16411. doi:10.1021/acsami.9b04383.

Spatial Patterning of Molecular Cues and Vascular Cells in Fully Integrated Hydrogel Channels *via* Interfacial Bioorthogonal Crosslinking

Kevin T. Dicker[1], **Axel C. Moore**[2], **Nikolay T. Garabedian**[3], **Han Zhang**[4], **Samuel L. Scinto**[4], **Robert E. Akins**[5], **David L. Burris**[3], **Joseph M. Fox**[1,4,*], and **Xinqiao Jia**[1,2,*]

[1]Department of Materials Science and Engineering, University of Delaware, Newark, DE, 19716, USA

[2]Department of Biomedical Engineering, University of Delaware, Newark, DE, 19716, USA

[3]Department of Mechanical Engineering, University of Delaware, Newark, DE 19716, USA

[4]Department of Chemistry and Biochemistry, University of Delaware, Newark, DE, 19716, USA

[5]Department of Biomedical Research, A.I. DuPont Hospital for Children, Nemours Children's Clinic, Wilmington, DE 19803, USA

Abstract

Fully integrated hydrogel channels were fabricated *via* interfacial bioorthogonal crosslinking — a diffusion-controlled method for the creation and patterning of synthetic matrices based on the rapid bioorthogonal reaction between *s*-tetrazines (Tz) and *trans*-cyclooctene (TCO) dienophiles. Injecting an aqueous solution of a bisTCO crosslinker into a reservoir of tetrazine-modified hyaluronic acid (HA-Tz), while simultaneously drawing the syringe needle through the reservoir, yielded a crosslinked hydrogel channel that was mechanically robust. Fluorescent tags and biochemical signals were spatially patterned in the channel wall through time-dependent perfusion of TCO-conjugated molecules into the lumen of the channel. Different cell populations were spatially encapsulated in the channel wall *via* temporal alteration of cells in the HA-Tz reservoir. The interfacial approach enabled spatial patterning of vascular cells, including human abdominal aorta endothelial cells, aortic vascular smooth muscle cells, and aortic adventitial fibroblasts, into the hydrogel channels with high viability and proper morphology in the anatomical order found in human arteries. The bioorthogonal platform does not rely on external triggers and represents a first step towards the engineering of functional and implantable arteries.

Graphical Abstract

*Corresponding authors: jmfox@udel.edu, xjia@udel.edu.

Supporting Information: Synthesis of SMR-bisTCO, construction of PDMS chamber, determination of gel stiffness via pressure dilation, bright field / confocal images of vascular cells cultured in hydrogel channels and confocal imaging conditions. This material is available free of charge via the Internet at http://pubs.acs.org.

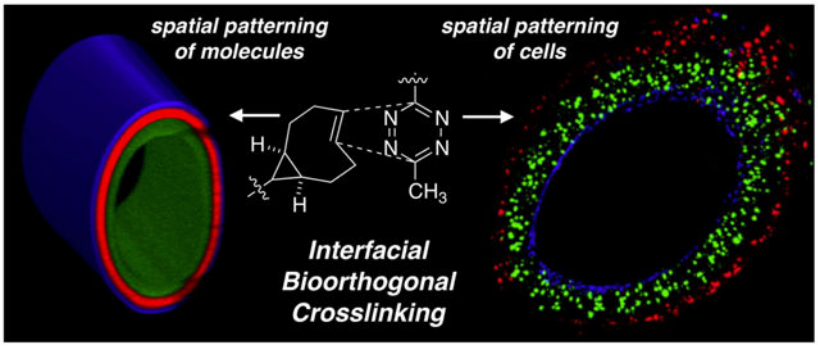

Keywords

tetrazine ligation; hydrogel channels; spatial patterning; arteries; vascular cells

1. Introduction

Cardiovascular disease is the leading cause of mortality in the United States, with nearly 33% of all deaths attributed to this disease.[1] Autologous or allogeneic arteries are commonly used in bypass surgeries to treat patients with severe vessel occlusion. Complications of such treatments include tissue shortage, donor site morbidity and immunological rejection.[2] Moreover, depending on the specific procedure, these implants fail at unacceptably high rates of up to 50% due to vessel wall remodeling and thickening caused by atherosclerosis or intimal hyperplasia.[3] Biomaterials-based, tissue-engineered blood vessels offer an attractive alternative for the treatment of cardiovascular disease.[4] For scaffolding materials, researchers have relied on natural extracellular matrix (ECM) proteins, such as collagen and fibrin, and synthetic polymers, such as polyesters and polyurethanes. The usage of animal derived products carries the risks of immunogenicity and disease transmission. Moreover, reconstituted protein gels are mechanically weak, thereby requiring synthetic polymers for reinforcement purposes. Synthetic polymers, on the other hand, are bioinert, thus requiring additional treatment to improve cell adhesion. Although polyesters generally have good biocompatibility, the breakdown products are acidic, which can invoke inflammatory responses and cellular toxicity.[5]

Using natural proteins or synthetic polymers, tubular structures are fabricated by rolling a sheet of polymer over a mandrel, crosslinking liquid precursor inside an annular mold, or electrospinning of polymer solution on the surface of a rotating cylinder.[6–10] Once fabricated, the scaffolds are seeded with cells found in the native vessels. Major blood vessels, such as arteries and veins, exhibit a unique trilayer structure, consisting of the tunica intima (the luminal side) with a cohesive endothelial cell monolayer, the tunica media (the middle layer) that is comprised of contractile smooth muscle cells and the tunica adventia (the outermost layer) that is sparsely populated with fibroblasts.[11] Under static seeding conditions, endothelial cells introduced into the graft settle stochastically onto the surface. Because smooth muscle cells introduced to the lumen do not penetrate deeply into the construct, centrifugal forces[12,13] or pressure gradients[14,15] have been applied to improve seeding efficiency. Such non-physiologic conditions can negatively affect cell viability and

distort cell morphology. Finally, additional casting has to be applied around the core structure to create the adventia.[16]

Alternative approaches that recapitulate the fundamental features of the vascular wall and enable *in situ* cell encapsulation during tube formation with precise localization of desired cell types in the intimal, medial and adventitial space in an integrated hydrogel is desirable. Facile fabrication of multilayered and multicellular vascular constructs requires the usage of highly efficient bioorthogonal reactions. Tetrazine ligation (Figure 1A) is a bioorthogonal reaction that exhibits rapid kinetics toward *trans*-cyclooctene (TCO) dienophiles ($k_2 > 10^5$ $M^{-1}s^{-1}$).[17,18] This chemistry has been applied to the fabrication and 3D molecular patterning of spherical hydrogels[17,19] and the synthesis of microfibers with cell guidance cues.[20–22] When combined with a complementary coupling reaction with a slower, bulk kinetics, tetrazine ligation has enabled *in situ* modification of the cellular microenvironment in 3D to modulate stem cell functions.[23] Previously, we also demonstrated that interfacial crosslinking *via* tetrazine ligation could be used to create water-filled hydrogel channels by drawing a solution of bisTCO through a reservoir of tetrazine modified hyaluronic acid (HA-Tz).[17] However, our initial method could only produce relatively soft channels that were difficult to manipulate. Consequently, spatial patterning of molecules and cells in the channel wall was challenging.

Described herein is a new method for creating hydrogel channels where cell guidance signals and different cell populations can be radially patterned in 3D. HA-Tz, with a high degree of modification, was synthesized using a 3-methyl-6-aryl tetrazine that is more water soluble than the diphenyl or dipyridyl tetrazine derivatives.[19] Mechanically robust hydrogel channels were prepared without the use of external triggers or templates employing an interfacial bioorthogonal crosslinking process (Figure 1B, C). Hydrogel channels were established by injecting TCO-derived crosslinkers into a solution of HA-Tz while simultaneously withdrawing the syringe needle. Channel formation was instantaneous owing to the rapid interfacial kinetics of the crosslinking chemistry. Subsequent co-diffusion of TCO-conjugated molecules allowed for spatially resolved patterning of fluorophores or biomolecules that modulate the local 3D microenvironment of encapsulated cells. By simply altering the cell type at different time points during the crosslinking process, it was possible to create radial patterns of different cell populations in the channel wall that reflect the anatomical order of the primary cell types found in human arteries.

2. Experimental Section.

2.1. General Information.

All reactions were carried out in glassware that was flame-dried under vacuum and cooled under nitrogen. Cy3-TCO and Cy5-TCO were purchased from AAT Bioquest (Sunnyvale, CA). O, 0'-Bis(2-aminoethyl)hexacosaethylene glycol (≥ 95% oligomer purity) was purchased from Santa Cruz Biotechnology (Dallas, TX). HA (sodium salt, 430 kDa) was a generous gift from Sanofi/Genzyme Corporation (Cambridge, MA). 2, 5-Dioxopyrrolidin-1-yl 2-(4-(6-methyl-1,2,4,5-tetrazin-3-yl)phenyl)acetate was purchased from Kerafast (Boston, MA). Reactive intermediates, including (rel-1R,8S,9R,4E)-bicyclo[6.1.0]non-4-ene-9-ylmethanol,[24] d-TCO-carbonate,[18] and 2-(4-(6-methyl-1,2,4,5-tetrazin-3-

yl)phenyl)acetohydrazide,[19] were prepared following known procedures. Dialysis membranes with a molecular weight cut-off (MWCO) of 10 kDa were purchased from Spectrum Labs (Waltham, MA). Flash chromatography was performed using normal phase Silicycle silica gel (40-63D, 60Å). Other reagents were purchased from commercial sources without additional purification.

2.2. Synthesis and Characterization of Hydrogel Channels.

2.2.1. Synthesis of hydrogel building blocks.—Following our established peptide synthesis protocol,[19] matrix metalloproteinase (MMP)-degradable peptide, with a sequence of Ac-GKRDVPM↓MRGGDRKG-NH_2 (abbreviated as SMR), was prepared using a CEM Liberty Blue Peptide Synthesizer (Matthews, NC), cleaved using standard TFA/TIPS/H_2O (95:2.5:2.5) cocktail and purified by HPLC (Waters, Milford, MA). To synthesize SMR-bisTCO (Scheme S1), SMR (144.2 mg, 80.6 μmol) was dissolved in anhydrous DMF (3 mL). *N, N*-Diisopropylethylamine (56.2 μL, 322 μmol) and dTCO-4-nitrophenyl carbonate[18] (70.4 mg, 202 μmol) were sequentially added to the DMF solution. The solution was stirred at room temperature for 2 h. The reaction was deemed complete when only the desired bifunctional product was observed by UPLC-MS. The resulting solution was added dropwise to 45 mL of ice-cold diethyl ether. The mixture was then centrifuged at 4,000 rpm for 5 mins, and the clear ethereal solution was removed. The solid was re-dissolved in 3 mL of DMF and precipitated into ice-cold diethyl ether. The precipitation/dissolution cycle was repeated for a total 3 times. An analytical grade sample was obtained by purification of the white powder by reverse phase chromatography on C_{18} silica gel using a gradient of 5% to 95% MeOH in neutral water. UPLC-MS for SMR-bisTCO: t_R = 1.79 mins, $[M+2H]^{2+}$ found 1105.11. UPLC-MS for SMR: t_R = 1.03 mins, $[M+4H]^{4+}$ found 447.99.

Other hydrogel building blocks, including HA-Tz,[19] poly(ethylene glycol)-based, non-degradable TCO crosslinker (PEG-bisTCO),[19] peptide-based (Ac-GKRDGPQG↓IWGQDRKG-NH_2), MMP-degradable TCO crosslinker (GIW-bisTCO),[19] TCO-tagged cell adhesive peptide (RGD-TCO),[20] Clover-TCO,[20] and Alexa-TCO[17] were prepared following our reported procedures. For 3D culture purposes, HA-Tz and all TCO-conjugated molecules were dissolved in PBS and sterile-filtered using a 0.22 μm poly(vinylidene fluoride) (PVDF) syringe filter (Thermo Fisher Scientific, Waltham, MA).

2.2.2. Channel formation.—HA-Tz (2 wt%), bisTCO crosslinker (PEG, GIW or SMR, 4.1 mM) and RGD-TCO (0.8 mM) were dissolved separately in PBS. HA-Tz (400 μL) was added to the well of a custom-made poly(dimethylsiloxane) (PDMS) chamber (Supporting Information, Figure S5) sitting on a moving stage. A syringe with a 21G (ID-0.514 mm, OD-0.819 mm) blunt needle (Component Supply Company, Fort Meade, FL) containing the bisTCO solution (500 μL) was placed in a syringe pump with the needle placed through the inlet and outlet of the PDMS chamber. The syringe needle was moved horizontally through the PDMS chamber while the bisTCO solution (20 μL) was injected into the HA-Tz bath over 13 s. The channel was allowed to crosslink further until the desired wall thickness was reached. The HA-Tz solution was removed and the channel was washed with PBS.

2.2.3. Mechanical analysis.—The hydrogel channels were allowed to crosslink for 5 min following the initial channel wall formation. PBS was then perfused through the channel and India ink (Super Black™) was added for visualization purposes. The surrounding HA-Tz solution was maintained to help support the weight of the channel and to maintain a hydrated environment. Once complete fluid communication was established, the chamber outlet was plugged with a Sticky-Tack polymer compound. This configuration established the reference state of the hydrogel channel. A digital camera with a calibrated magnifier (Dino-Lite AM7915MZTL) was centered overtop of the channel and the field of view was set such that the entire hydrogel channel could be observed. To control for the optical effects of the fluid meniscus, a flat glass slide was placed on top of the fluid filled chamber. To mechanically characterize the hydrogel channels, a pressure-dilation assay was conducted (Supporting Information). Under the experimental configuration, pressure was determined based on the distance in which the screw-driven head tank moved relative to the stationary hydrogel channel (Figure 2A). Young's modulus was calculated according to a mechanical model that described the change in diameter as a function of pressure. The change in channel dilation, in response to the change in fluid pressure, was tracked by taking consecutive microscope images. A custom edge detection code was written in MatLab® to identify the channel boundaries and measure the radial changes. The contrast provided by the India ink saline solution allowed the algorithm to construct a bimodal distributed histogram of the pixel intensity across the image and separate the darker areas which were representative of the inner diameter of the channel. Because the channels were attached to the PDMS chamber at both the inlet and outlet, which likely created edge effects, only the dilation in the central 30% was monitored.

2.2.4. Covalent patterning of fluorophores.—HA-Tz (2 wt% PBS) was added to the PDMS chamber well. A syringe containing PEG-bisTCO (4.4 mM) and Clover-TCO (5 μM) was drawn through the well while ~20 μL of solution was injected as described above. The channel was allowed to crosslink for 5 min before fresh PBS was perfused through the channel. A solution of PEG-bisTCO (4.4 mM) and Cy3-TCO (5 μM) was injected into the lumen of the channel and allowed to crosslink for 15 min. The channel was flushed with fresh PBS before a solution of PEG-bisTCO (4.4 mM) and Cy5-TCO (5 μM) was injected into the lumen of the channel. After 45 min incubation, the channels were washed with PBS overnight before imaging using a Zeiss 710 NLO confocal microscope with a 5× objective.

2.3. Cell Maintenance and 3D culture

2.3.1. Cell maintenance.—NIH3T3 fibroblasts (ATCC, Manassas, VA) were maintained in a Dulbecco's modified eagle medium (DMEM, Corning Inc., Corning, NY) supplemented with 10% fetal bovine serum (FBS) and 1% penicillin-streptomycin (PS). Green fluorescent protein-labeled fibroblasts (NIH3T3-GFP, Cell Biolabs, San Diego, CA) were maintained in a DMEM medium supplemented with 10% FBS, 0.1 mM MEM non-essential amino acids (NEAA) and 1% PS. Human abdominal aorta endothelial cells (HAAE, ATCC, Manassas, VA) cells were maintained in a F-12K medium (ATCC, Manassas, VA) supplemented with heparin (0.1 mg/mL), endothelial cell growth supplement (ECGS, 0.03 mg/mL), FBS (10%), and PS (1%). Human aortic vascular smooth muscle cells (vSMCs, ATCC, Manassas, VA) were maintained in a F-12K medium supplemented with N-

tris (hydroxymethyl) methyl-2-amino-ethanesulfonic acid (TES, 10 mM), and N-2-hydroxyethyl- oioerazine-N'-2-ethanesulfonic acid (HEPES, 10 mM), ascorbic acid (0.05 mg/mL), sodium selenite (10 ng/mL), transferrin (0.01 mg/mL), ECGS (0.03 mg/mL), insulin (0.01 mg/mL), FBS (10%), and PS (1%). Human aortic adventitial fibroblasts (AoAFs, Lonza, Walkersville, MD) were maintained in a stromal cell growth medium BulletKit (Lonza, Walkersville, MD). Media was refreshed every other day.

2.3.2. Fibroblast culture in patterned matrix.—NIH3T3-GFP fibroblasts were dispersed (2×10^6/mL) in HA-Tz (2 wt% in PBS) and added to the well of the PDMS chamber as described above. A TCO solution (20 μL) containing PEG-bisTCO (5 mM) and Alexa-TCO (2 μM) was injected into the chamber through a syringe. The channel was incubated for 5 min before being flushed with PBS. Next, a solution of GIW-bisTCO (3.2 mM) and RGD-TCO (0.4 mM) was perfused into the channel. After 15 min incubation, the channel was flushed with PBS before a fresh solution of PEG-bisTCO (5 mM) and Alexa-TCO (2 μM) was perfused into the channel. After 30 min incubation, the HA-Tz bath containing suspended cells was removed and the chamber was washed with PBS. The channels were transferred to wells containing fresh media and were incubated at 37°C for up to 28 days, with media refreshed every other day.

2.3.3. 3D patterning of fibroblasts.—Prior to encapsulation, NIH3T3 fibroblasts were stained with either Cell Tracker Red CMTPX (10 μM) or Cell Tracker Green CMFDA (10 μM) (Thermo Fisher, Waltham, MA) for 30 min. The red cells were dispersed (2×10^6/mL) in HA-Tz (2 wt% in PBS) and added to the well of the PDMS chamber. A syringe containing PEG-bisTCO (5 mM) was drawn through the chamber, injecting 20 μL of crosslinking solution. After 5 min incubation, the red cell bath was removed and the chamber was washed with PBS. HA-Tz (2 wt% in PBS) containing dispersed green cells (2×10^6/mL) was introduced to the chamber well and the interfacial reaction was allowed to proceed for 15 min. Upon removal of the green cell bath followed by PBS wash, HA-Tz containing dispersed red cells was returned to the chamber and the reaction was allowed to proceed for 45 min. The PEG-bisTCO crosslinker in the lumen of the channel was replenished throughout the experiment. After the red cell bath was removed and the chamber was washed with PBS, the cell-laden channels were transferred to a 4-well Nunc chamber (Thermo-Fisher, Waltham, MA) containing fresh media and imaged immediately using a Zeiss 710 NLO confocal microscope with a 5× objective. Top down images were taken of 1-mm rings cut from the channel with a scalpel.

2.3.4. 3D patterning of vascular cells.—Prior to 3D patterning, vSMCs, AoAFs and HAAEs were stained for 30 min at 37°C with cell tracker green (10 μM), red (10 μM) and deep red (1 μM), respectively. vSMCs and AoAFs were dispersed (2×10^6 cells/mL) in HA-Tz (2 wt% in PBS) baths separately. vSMC bath (250 μL) was added to the well of the PDMS chamber. The initial channel wall was established as described above for 5 min with a crosslinking solution of SMR-bisTCO (4.1 mM) and RGD-TCO (0.8 mM). The vSMC bath was removed and replaced with the AoAF bath after replenishing the crosslinker in the lumen of the channel via perfusion. The chamber was incubated for 30 min under longitudinal rotation. The AoAF bath surrounding the channel was replaced with a liquid

prepared by mixing the cell type specific medium at a volumetric ratio of 1:1:1. Finally, HAAEs (8×10^6 cells/mL, 50 μL) were perfused into the channel and the cellular construct was maintained at 37°C in mixed media overnight. Channels were imaged after 24 h of culture using a Zeiss 710 NLO confocal microscope with a 5× objective. Cellular constructs containing one vascular cell type were prepared similarly and incubated at 37°C for up to 7 days, with media refreshed every other day.

2.3.5. Cell viability and cell morphology.—Percent cell viability was assessed by Live/Dead staining with calcein AM and ethidium homodimer after 7 days of culture. Short z-stacks of 225 μm with 15 slices were taken with Zeiss 710 NLO confocal microscope with a 5× objective. The images were flattened in Zeiss's Zen software to produce maximum intensity projections. Using Image J, live and dead cells were enumerated in each image, and the percent viability was quantified. Values are presented as a percentage of live cells compared with the total number of cells.[19] Encapsulated cells were subsequently stained for F-actin using Alexa Fluor 568-conjugated phalloidin and with the nuclei counter stained by DAPI, following our previous protocols.[25] Stained samples were imaged using a Zeiss 710 NLO confocal microscope with a 40× objective.

3. Results and Discussion

3.1. Channel Fabrication.

HA, a non-sulfated glycosaminoglycan found in the natural ECM surrounding vascular cells,[26] was allowed to react with hydrazide-functionalized methylphenyl tetrazine (Tz-hydrazide) to afford HA-Tz (Figure 1A) with 18.6% tetrazine incorporation.[19] Separately, a non-degradable TOO crosslinker (PEG-bisTCO: 1,608 Da) was synthesized using defined length PEG_{27} diamine. MMP sensitive peptides, with a sequence of VPMS↓MRGG (SMR) or GPQG↓IWGQ (GIW), flanked with GKRD residues, were produced via solid-state peptide synthesis. Aspartic acid (D) and arginine (R) residues were introduced to improve aqueous solubility while the lysine (K) amine was used for covalent conjugation of TCO to form bifunctional crosslinkers (GIW-bisTCO: 2,218 Da;[19] SMR-bisTCO: 2,208 Da, Figure S1-4). Although both peptides are susceptible to cleavage by MMP-1, 2, 3, 8 and 9, SMR exhibits faster degradation kinetics than GIW.[27,28] To introduce integrin binding sites in the crosslinked network, TCO was conjugated to a fibronectin-derived peptide sequence, RGDSPG (RGD), to form a monofunctional linker RGD-TCO (1,269 Da).[20]

Covalently crosslinked hydrogel channels were fabricated using a custom-made PDMS chamber (Figure S5) by injecting the bisTCO crosslinker solution into a reservoir of HA-Tz using a 21G syringe while simultaneously moving the syringe unidirectionally through the chamber (Figure 1C). Methylphenyl tetrazine reacts with strained *trans*-cyclooctenes, *s*-TCO and *d*-TCO, at a rate faster than molecular diffusion through crosslinked gel networks, with a second order rate constant, k_2, of 6.70×10^4 $M^{-1}s^{-1}$ and 9.94×10^3 $M^{-1}s^{-1}$, respectively.[19] Therefore, when bisTCO was exposed to HA-Tz following the path of the syringe needle, a crosslinked wall formed instantaneously at the interface between the two liquids. The smaller bisTCO molecules diffused through the crosslinked wall and reacted with high molecular weight HA-Tz at the gel-liquid interface, growing the crosslinked channel wall

outward radially. The spent TCO species could be replenished with perfusion of a fresh crosslinker solution into the lumen of the channel. Thus, the thickness of the channel wall was a function of reaction time. When the desired wall thickness was reached, the crosslinking reaction was terminated by the perfusion of fresh PBS to flush unreacted TCO species from the lumen of the channel. We did not observe any nitrogen gas bubbles trapped in the bulk of the gel matrix because the reaction occurred at the gel/liquid interface, allowing rapid escape of the gaseous byproduct.

The mechanical properties of the hydrogel channels were analyzed by a pressure-dilation assay (Figure 2A and Figure S6-7). This method employs the most physiologically relevant testing configuration and provides straightforward interpretation of the mechanical properties of the hydrogel channels. The thickness of each channel was measured by selecting the uniform medium contrast zone surrounding the India ink (a black dye) filled interior of the channels, visible in the optical micrographs. A thin-walled pressure vessel model was used to quantify the Young's modulus at each pressure-diameter pair for each channel tested. Reported moduli represent the mean and standard deviation of range of moduli obtained for each sample (Figure 2B). The Young's modulus was found to be 1.2 ± 0.1 kPa to 2.8 ± 0.6 kPa for applied pressures of 0 to 150 Pa. Reported moduli for native arteries are significantly higher (up to 10 MPa), owing to the presence of load bearing fibrous proteins, such as elastin and collagen, and various cellular components.[29,30]

3.2. Spatial Patterning of Molecular Cues and Fibroblasts.

We envisioned that radially-patterned hydrogel channels could be fabricated, as outlined in Figure 3, *via* sequential injection of crosslinkers containing bioorthogonal capping groups. In an initial experiment, a fluorescently-patterned channel was created through sequential injections of TCO-capped fluorophores that included both small molecule chromophores as well as a site-selectively tagged fluorescent protein. Thus, a PEG-bisTCO (4.4 mM) solution containing 5 μM Clover-TCO[20] was injected to the HA-Tz reservoir (Figure 3A). After 5 min, a bisTCO solution containing 5 μM Cy3-TCO was perfused into the channel and the channel was maintained at ambient temperature for 15 min (Figure 3B). Finally, the Cy3-TCO crosslinking solution was replaced with one containing Cy5-TCO (5 μM) and the reaction was allowed to proceed for an additional 45 min (Figure 3C). As shown in Figure 3D-G, the crosslinked channel wall displayed a trilayer structure, with the innermost layer stained green by Clover, the middle layer stained red by Cy3 and the outermost layer stained blue by Cy5. From the luminal side outwards, individual layers had an average thickness of 134 ± 14, 75 ± 5 and 57 ± 3 μm. Because tetrazine ligation is highly efficient and the TCO groups were in excess relative to the tetrazine functionalities at the gel/liquid interface, all tetrazine groups were consumed during crosslinking[19] as the gel-liquid interface moved outward from the lumen. Consequently, the boundaries between adjacent layers were sharp and distinct. This result confirmed that temporal alteration of the TCO solution composition led to the spatial patterning of TCO conjugated molecules through the channel wall. It is noteworthy that the concentration of HA-Tz and PEG-bisTCO was maintained constant throughout the crosslinking process, and the concentration of TCO dyes was minute compared to that of the bisTCO crosslinker. Therefore, it is unlikely that the mechanical property of individual layers within the channel wall would vary. However, spatial

modulation of matrix stiffness is possible and can be achieved by varying the ratio of mono-functional and bi-functional TCO molecules during the interfacial crosslinking process.[19]

The diffusion-controlled approach also enables 3D patterning of peptidic molecules that can mediate cellular behavior. To demonstrate that interfacial bioorthogonal chemistry can be used to create 3D-patterns of cell adhesive ligands, hydrogel channels containing a MMP-degradable (GIW) and RGD-decorated middle layer sandwiched between two peptide-free regions were prepared for 3D culture of NIH 3T3 fibroblasts (Figure 4A-D). The inner and the outer walls were established using the bioinert crosslinker (PEG-bisTCO) along with Alexa-TCO[17] for visualization. After the PEG-bisTCO and Alexa-TCO solution had been incubated for 5 min, a peptide solution (3.2 mM GIW-bisTCO and 0.4 mM RGD-TCO) was perfused into the lumen of the channel. After 5 min, the bioinert crosslinking solution was again perfused into the lumen and the channel was incubated for 45 min (Figure 4A, B). This formulation leads to the construction of a tri-layer structure within the hydrogel channel wall in the radial direction. In this experiment, fibroblasts transfected with GFP were dispersed in the HA-Tz reservoir during the entire 65 min, and therefore were encapsulated homogeneously in the channel wall.

Confocal images were acquired from a vertically positioned ring (1 mm thick) cut from the mid-portion of the channel using a surgical scalpel. As shown in Figure 4C, fibroblasts residing in the peptide-free regions (stained blue with Alexa-TCO) remain round after 7 days of culture, whereas those in the peptide-containing middle region (without any stain, black) had started to adopt a spindle-like morphology. More dead cells (stained red by ethidium homodimer) were present in the peptide-free regions than in the cell-adhesive, MMP-degradable regions. After 28 days of culture (Figure 4D), cells in the middle layer proliferated and made cell-cell connections. By contrast, cells in the inner/outer blue layers remained rounded, with a significant decrease in the expression of GFP, indicating compromised cell functions.[31] Our observation highlights the importance of the reciprocal cell-matrix interaction for the maintenance of proper cell functions.[32,33] In agreement with our previous reports,[19] although fibroblasts can potentially interact with HA through cell surface receptors CD44 and RHAMM, such binding is not sufficient to promote cell attachment, spreading and proliferation in 3D in covalently crosslinked HA gels. Integrin-binding and MMP-degradable peptidic motifs are necessary to elicit significant morphological changes through the development of cytoskeletal stress fibers.

Next, we investigated whether the interfacial crosslinking platform could be used for spatial patterning of living cells. To this end, fibroblasts labeled with either cell tracker red or cell tracker green were dispersed in separate HA-Tz reservoirs. The red cell reservoir was first added to the PDMS chamber for the formation of the initial channel wall. After 5 min, the red cell reservoir was replaced with the green cell reservoir and the crosslinking solution in the lumen of the channel was replenished via perfusion. The channel was incubated for 15 min. Finally, the green cell reservoir was removed and the initial red cell reservoir was returned to the chamber well for an additional 45 min incubation period (Figure 4E, F). As shown in Figure 4G, a trilayer construct with alternating layers of red and green cells was produced and the spatial pattern reflects the order in which the cells were introduced to the chamber.

3.3. Spatial Patterning of Vascular Cells.

Having confirmed the utility of the interfacial crosslinking approach for 3D patterning of fluorophores, peptides and fibroblasts, we explored the applicability of such method for the establishment of a fully integrated channel containing encapsulated vascular cells. As mentioned above, the arterial wall is a multilayered structure, comprised of three primary cell types in a distinct radial order. Vascular endothelial cells form a barrier between the circulating blood and the arterial wall and secrete cell signaling molecules such as vasodilators and vasoconstrictors.[34] Vascular smooth muscle cells control blood pressure and flow by contraction and dilation.[35] Adventitial fibroblasts help to maintain the overall vessel integrity and participate in the remodeling of the vessel wall.[36] In order to fabricate a viable *in vitro* vascular model, these three cell types must be presented in the distinct radial order found *in vivo.*

The cytocompatibility of the hydrogel formulation was tested using the three vascular cell types separately. In this experiment, the hydrogel channel was prepared using a crosslinking solution of SMR-bisTCO (4.1 mM) and RGD-TCO (0.8 mM). SMR-bisTCO was used in place of GIW-bisTCO as the MMP substrate to promote rapid cell spreading in 3D.[37] HAAEs were perfused into the lumen of the channel after 5 min of crosslinking and the constructs were incubated overnight at 37 °C to allow for cells to attach to the inner channel wall of the lumen. Initially, HAAEs attached to the channel on the bottom portion of the inner wall due to gravity. Over a 7 day period, cells formed a monolayer and completely covered the inner wall, maintaining a high viability (98%, Figure 5A-D). Separately, AoAFs were dispersed in the HA-Tz reservoir and encapsulated into the hydrogel channel wall during 5 min of crosslinking. vSMCs were similarly encapsulated in a separate experiment. Initially, both AoAFs and vSMCs were round and dispersed (Figure S8), but after 7 days of culture adopted an elongated shape (Figure 5E-L) with high viability (96% and 92% for vSMCs and AoAFs, respectively, Figure S9) while encapsulated in the channel. In all three experiments, cells were able to attach to the synthetic matrix and alter their morphology (Figure 5D, H, L) from an initial rounded state to a spread-out morphology with mature stress fibers traversing the entire cell body, indicative of cell attachment and appropriate cell function.[11]

Finally, HAAEs, vSMCs, and AoAFs were spatially patterned into the hydrogel channel in the anatomical order found *in vivo* (Figure 5M-Q). vSMCs, tagged with cell tracker green, were dispersed in the HA-Tz reservoir and crosslinked into the initial channel wall with a 5 min incubation period, generating a cell-laden medial layer with a thickness of 151.9 ± 29.0 μm. The vSMC reservoir was removed and the chamber was filled with a HA-Tz solution containing dispersed AoAFs tagged with cell tracker red. The lumen of the channel was replenished with additional SMR-bisTCO and RGD-TCO and the channel wall was allowed to crosslink for another 30 min. The resultant adventitial layer had a thickness of 74.5 ± 23.9 μm. Finally, HAAEs stained blue with cell tracker deep red were perfused into the lumen of the channel and allowed to attach to the inner channel wall overnight at 37 °C under gentle rotation to ensure the establishment of a homogenous cell layer. After 24 h, the cell-laden hydrogel channels were examined by confocal microscopy for spatial presentation of the fluorescently tagged cells. As shown in Figure 5M-Q, cells were layered in the correct

anatomical order according to the experimental setup. As shown in side profiles in Figure 5O-Q, cells were homogeneously dispersed and the channel wall increased in thickness progressively from the HAAEs region (Figure 5O) to the vSMCs region (Figure 5P) and finally to the AoAFs on the outer layer of the channel (Figure 5Q).

Collectively, the diffusion-controlled bioorthogonal platform offers a new strategy to spatially pattern all three vascular cell types without the need for multiple separate gelation steps and concentric needles.[8] This work represents a first step towards a functional and implantable artery. The diameter of major arteries in the human body is in the millimeter size range, and individual layers within the arterial wall are tens to hundreds of microns thick.[38] Because the tetrazine/TCO reaction is instantaneous, the width of the hydrogel channel can be tuned by varying the diameter of the syringe needle used to inject the bisTCO solution. Because crosslinking is diffusion-controlled, the thickness of the channel wall, as well as that of the individual layers within the wall, can be modulated by terminating the interfacial reaction at different time points, as long as there is sufficient amount of bisTCO in the lumen. This is the subject of our current investigation. Additional studies will focus on culturing the cellularized channel in the presence of physiologically relevant mechanical stimulations, including pulsatile fluid flow, cyclic strain and shear stress. The mechanical conditioning is likely to preserve the cell phenotype, improve cell function and promote tissue maturation, ultimately giving rise to a physiologically relevant construct with tissue-like mechanical and haemodynamic properties. To this end, we are developing immunohistochemistry and *in situ* hybridization methods to analyze the spatial distribution of cell-specific proteins and markers.

4. Conclusion

In summary, we have demonstrated the utility of tetrazine ligation as a powerful tool for fabrication of fully integrated hydrogel channels via interfacial diffusion-controlled crosslinking. The hydrogel channels were spatially patterned with peptides to modulate the 3D microenvironment. The hydrogel channels were also spatially patterned with different cell populations in distinct orders. The ability and relative ease of spatially patterning both biochemical cues and multiple relevant cell populations into the hydrogel channel makes this an ideal platform for the fabrication of *in vitro* vasculature models and functional implants.

Supplementary Material

Refer to Web version on PubMed Central for supplementary material.

Acknowledgements:

This work was supported in part by National Institutes of Health (NIH, R01 DC014461, R01 HL108110) and National Science Foundation (NSF, DMR 1506613, 1809612). Instrumentation was supported by grants from NIH (P30GM110758, P20GM104316, S10RR026962, S10OD016267) and NSF (CHE, 0840401, 1229234, and 1048367). We thank Sanofi/Genzyme for generously providing HA. We thank Dr. Rebecca Scott and Karyn Robinson for helpful discussions on 3D culture of vascular cells.

References

(1). American Heart Association. Heart Disease and Stroke Statistics; 2017.

(2). Pashneh-Tala S; MacNeil S; Claeyssens F The Tissue-Engineered Vascular Graft—Past, Present, and Future. Tissue Eng. Part B Rev. 2015, 22, 68–100. [PubMed: 26447530]

(3). FitzGibbon GM; Kafka HP; Leach AJ; Keon WJ; Hooper GD; Burton JR Coronary Bypass Graft Fate And Patient Outcome: Angiographic Follow-Up Of 5,065 Grafts Related To Survival And Reoperation In 1,388 Patients During 25 Years. J. Am. Coll. Cardiol. 1996, 28, 616–626. [PubMed: 8772748]

(4). Zhang WJ; Liu W; Cui L; Cao Y Tissue Engineering of Blood Vessel. J. Cell. Mol. Med. 2007, 11, 945–957. [PubMed: 17979876]

(5). Ravi S; Chaikof E Biomaterials for Vascular Tissue Engineering. Regen. Med. 2010, 5, 1–21. [PubMed: 20017686]

(6). Hasan A; Paul A; Vrana NE; Zhao X; Memic A; Hwang YS; Dokmeci MR; Khademhosseini A Microfluidic Techniques for Development of 3D Vascularized Tissue. Biomaterials 2014, 35, 7308–7325. [PubMed: 24906345]

(7). Sadr N; Zhu M; Osaki T; Kakegawa T; Yang Y; Moretti M; Fukuda J; Khademhosseini A SAM-Based Cell Transfer to Photopatterned Hydrogels for Microengineering Vascular-like Structures. Biomaterials 2011, 32, 7479–7490. [PubMed: 21802723]

(8). Hasan A; Paul A; Memic A; Khademhosseini A A Multilayered Microfluidic Blood Vessel-like Structure. Biomed. Microdevices 2015, 17, 1–13. [PubMed: 25653054]

(9). Hasan A; Memic A; Annabi N; Hossain M; Paul A; Dokmeci MR; Dehghani F; Khademhosseini A Electrospun Scaffolds for Tissue Engineering of Vascular Grafts. Acta Biomater. 2014, 10, 11–25. [PubMed: 23973391]

(10). Xing Q; Qian Z; Tahtinen M; Yap AH; Yates K; Zhao F Aligned Nanofibrous Cell-Derived Extracellular Matrix for Anisotropic Vascular Graft Construction. Adv. Healthc. Mater. 2017, 6, 1601333.

(11). Robinson KG; Nie T; Baldwin AD; Yang EC; Kiick KL; Akins RE Differential Effects of Substrate Modulus on Human Vascular Endothelial, Smooth Muscle, and Fibroblastic Cells. J. Biomed. Mater. Res. - Part A 2012, 100 A, 1356–1367.

(12). Nasseri BA; Pomerantseva I; Kaazempur-Mofrad MR; Sutherland FWH; Perry T; Ochoa E; Thompson CA; Mayer JE; Oesterle SN; Vacanti JP Dynamic Rotational Seeding and Cell Culture System for Vascular Tube Formation. Tissue Eng. 2003, 9, 291–299. [PubMed: 12740091]

(13). Hsu S; Tsai I; Lin D; Chen DC The Effect of Dynamic Culture Conditions on Endothelial Cell Seeding and Retention on Small Diameter Polyurethane Vascular Grafts. Med. Eng. Phys. 2005, 27, 267–272. [PubMed: 15694611]

(14). van Wachem PB; Stronck JW; Koers-Zuideveld R; Dijk F; Wildevuur CR Vacuum Cell Seeding: A New Method for the Fast Application of an Evenly Distributed Cell Layer on Porous Vascular Grafts. Biomaterials 1990, 11, 602–606. [PubMed: 2279063]

(15). Williams C; Wick TM Perfusion Bioreactor for Small Diameter Tissue-Engineered Arteries. Tissue Eng. 2004, 10, 930–941. [PubMed: 15265311]

(16). Song H; Rumma R; Ozaki C; Edelman E; Chen C Vascular Tissue Engineering: Progress, Challenges, and Clinical Promise. Cell Stem Cell 2018, 22, 340–354. [PubMed: 29499152]

(17). Zhang H; Dicker KT; Xu X; Jia X; Fox JM Interfacial Bioorthogonal Cross-Linking. ACS Macro Lett. 2014, 3, 727–731. [PubMed: 25177528]

(18). Darko A; Wallace S; Dmitrenko O; Machovina MM; Mehl RA; Chin JW; Fox JM Conformationally Strained Trans-Cyclooctene with Improved Stability and Excellent Reactivity in Tetrazine Ligation. Chem. Sci. 2014, 5, 3770–3776. [PubMed: 26113970]

(19). Dicker KT; Song J; Moore AC; Zhang H; Li Y; Burris DL; Jia X; Fox JM Core–shell Patterning of Synthetic Hydrogels via Interfacial Bioorthogonal Chemistry for Spatial Control of Stem Cell Behavior. Chem. Sci. 2018, 9, 5394–5404. [PubMed: 30009011]

(20). Zhang H; Trout WS; Liu S; Andrade GA; Hudson DA; Scinto SL; Dicker KT; Li Y; Lazouski N; Rosenthal J; Thorpe C; Jia X; Fox JM Rapid Bioorthogonal Chemistry Turn-on through Enzymatic or Long Wavelength Photocatalytic Activation of Tetrazine Ligation. J. Am. Chem. Soc. 2016, 138, 5978–5983. [PubMed: 27078610]

(21). Liu S; Zhang H; Remy RA; Deng F; Mackay ME; Fox JM; Jia X Meter-Long Multiblock Copolymer Microfibers Via Interfacial Bioorthogonal Polymerization. Adv. Mater. 2015, 27, 2783–2790. [PubMed: 25824805]

(22). Liu S; Moore AC; Zerdoum AB; Zhang H; Scinto SL; Zhang H; Gong L; Burris DL; Rajasekaran AK; Fox JM; Jia X Cellular Interactions with Hydrogel Microfibers Synthesized via Interfacial Tetrazine Ligation. Biomaterials 2018, 180, 24–35. [PubMed: 30014964]

(23). Hao Y; Song J; Ravikrishnan A; Dicker KT; Fowler EW; Zerdoum AB; Li Y; Zhang H; Rajasekaran AK; Fox JM; Jia X Rapid Bioorthogonal Chemistry Enables in Situ Modulation of the Stem Cell Behavior in 3D without External Triggers. ACS Appl. Mater. Interfaces 2018, 10, 26016–26027. [PubMed: 30015482]

(24). Taylor MT; Blackman ML; Dmitrenko O; Fox JM Design and Synthesis of Highly Reactive Dienophiles for the Tetrazine-Trans-Cyclooctene Ligation. J. Am. Chem. Soc. 2011, 133, 9646–9649. [PubMed: 21599005]

(25). Xu X; Gurski L. a; Zhang C; Harrington D. a; Farach-Carson MC; Jia X. Recreating the Tumor Microenvironment in a Bilayer, Hyaluronic Acid Hydrogel Construct for the Growth of Prostate Cancer Spheroids. Biomaterials 2012, 33, 9049–9060. [PubMed: 22999468]

(26). Dicker KT; Gurski LA; Pradhan-Bhatt S; Witt RL; Farach-Carson MC; Jia X Hyaluronan: A Simple Polysaccharide with Diverse Biological Functions. Acta Biomater. 2014, 10, 1558–1570. [PubMed: 24361428]

(27). Patterson J; Hubbell JA Enhanced Proteolytic Degradation of Molecularly Engineered PEG Hydrogels in Response to MMP-1 and MMP-2. Biomaterials 2010, 31, 7836–7845. [PubMed: 20667588]

(28). Nagase H; Fields GB Human Matrix Metalloproteinase Specificity Studies Using Collagen Sequence-Based Synthetic Peptides. Biopolymers 1996, 40, 399–416. [PubMed: 8765610]

(29). Hayashi K Experimental Approaches on Measuring the Mechanical Properties and Constitutive Laws of Arterial Walls. J. Biomech. Eng. 1993, 115, 481–488. [PubMed: 8302029]

(30). Hasan A; Ragaert K; Swieszkowski W; Selimović Š; Paul A; Camci-Unal G; Mofrad MRK; Khademhosseini A Biomechanical Properties of Native and Tissue Engineered Heart Valve Constructs. J. Biomech. 2014, 47, 1949–1963. [PubMed: 24290137]

(31). Steff A-M; Fortin M; Arguin C; Hugo P Detection of a Decrease in Green Fluorescent Protein Fluorescence for the Monitoring of Cell Death: An Assay Amenable to High-Throughput Screening. Cytometry 2001, 45, 237–243. [PubMed: 11746092]

(32). Lutolf MP; Raeber GP; Zisch AH; Tirelli N; Hubbell JA Cell-Responsive Synthetic Hydrogels. Adv. Mater. 2003, 15, 888–892.

(33). Nuttelman CR; Mortisen DJ; Henry SM; Anseth KS Attachment of Fibronectin to Poly(Vinyl Alcohol) Hydrogels Promotes NIH3T3 Cell Adhesion, Proliferation, and Migration. J. Biomed. Mater. Res. 2001, 57, 217–223. [PubMed: 11484184]

(34). Chlen S; Li S; Shyy J Effects of Mechanical Forces on Signal Transduction Gene Expression in Endothelial. Hypertension 1998, 31, 162–169. [PubMed: 9453297]

(35). Stegemann JP; Hong H; Nerem RM Mechanical, Biochemical, and Extracellular Matrix Effects on Vascular Smooth Muscle Cell Phenotype. J Appl Physiol 2005, 98, 2321–2327. [PubMed: 15894540]

(36). Sartore S; Chiavegato A; Faggin E; Franch R; Puato M; Ausoni S; Pauletto P Contribution of Adventitial Fibroblasts to Neointima Formation and Vascular Remodeling: From Innocent Bystander to Active Participant. Circ. Res. 2001, 89, 1111–1121. [PubMed: 11739275]

(37). Lin L; Marchant RE; Zhu J; Kottke-Marchant K Extracellular Matrix-Mimetic Poly(Ethylene Glycol) Hydrogels Engineered to Regulate Smooth Muscle Cell Proliferation in 3-D. Acta Biomater. 2014, 10, 5106–5115. [PubMed: 25173839]

(38). Mallery JA; Tobis JM; Griffith J; Gessert J; McRae M; Moussabeck O; Bessen M; Moriuchi M; Henry WL Assessment of Normal and Atherosclerotic Arterial Wall Thickness with an Intravascular Ultrasound Imaging Catheter. Am. Heart J. 1990, 119, 1392–1400. [PubMed: 2191579]

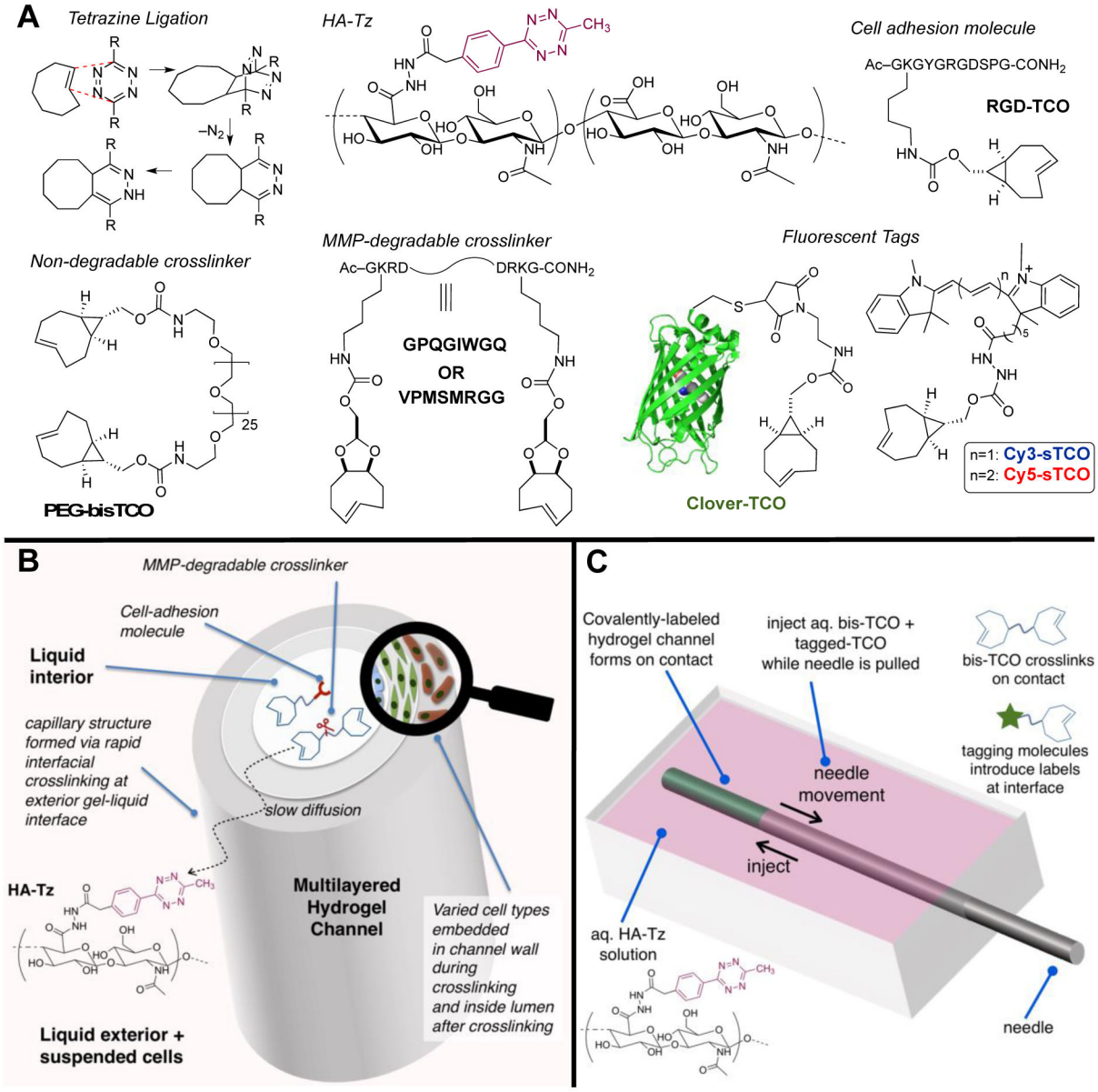

Figure 1.

Interfacial bioorthogonal approach to multicellular, multilayered hydrogel channels. **(A):** The inverse electron demand Diels-Alder reaction between *s*-tetrazine and TCO proceeds at a rate faster than molecular diffusion through the crosslinked network. Hydrogel building blocks included HA-Tz, non-degradable (PEG) and MMP-degradable bisTCO crosslinkers (GIW or SMR) and TCO-tagged integrin binding peptide (RGD-TCO). Fluorescent TCO conjugates were used to validate the spatial patterns. **(B):** Interfacial bioorthogonal crosslinking enabled spatial sequestration of three vascular cell types in an anatomical order during channel formation. **(C):** Channels were produced by injecting the bisTCO crosslinker solution to a reservoir of HA-Tz while removing the syringe needle simultaneously. Subsequent diffusion of TCO species through the crosslinked channel wall introduced further crosslinking at the gel-liquid interface.

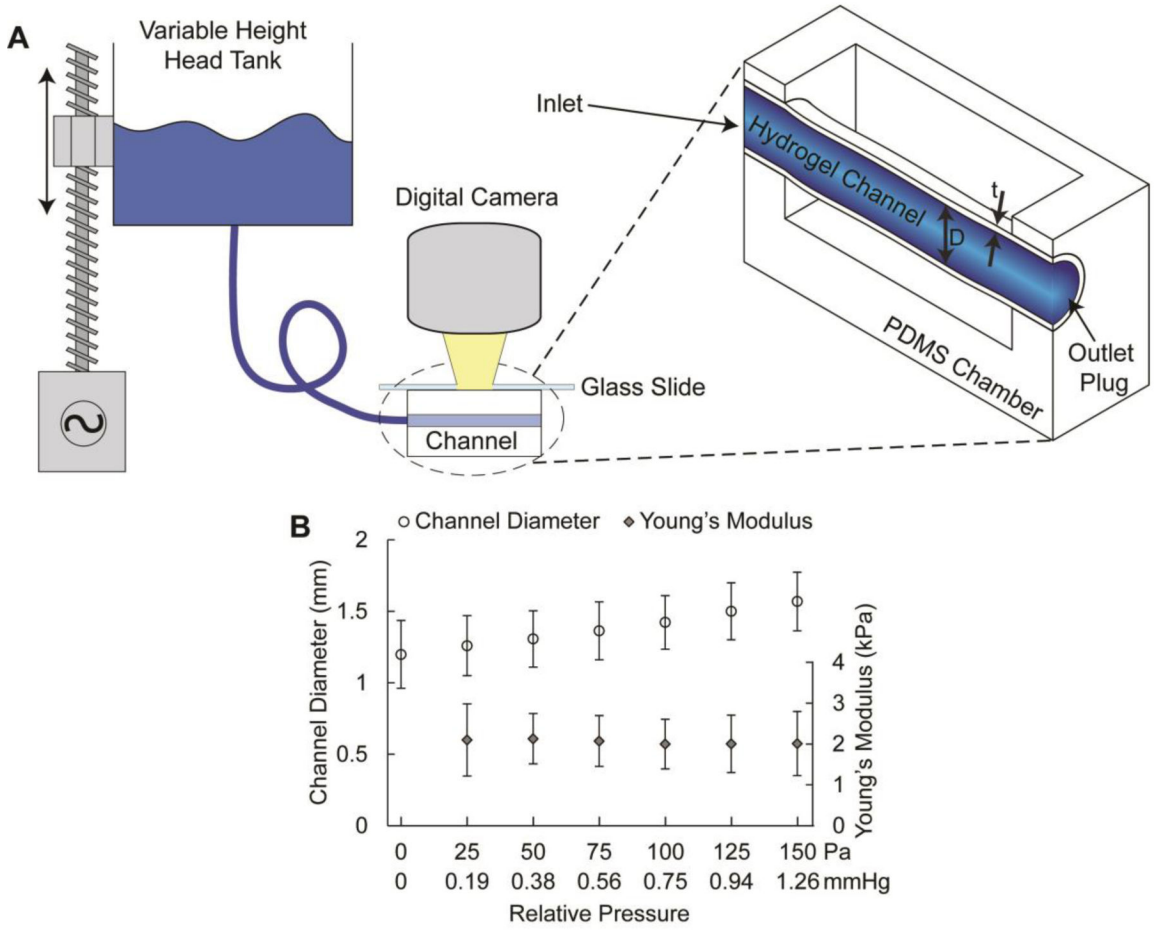

Figure 2.

Mechanical properties of hydrogel channels. **(A):** Schematic for pressure-dilation experiments on hydrogel channels. The head tank was driven by a linear actuator in 2.54 mm increments. An FEP tubing connected the head tank to one end of the PDMS chamber while the outlet was plugged. The chamber well was filled with HA-Tz and topped with a glass slide to prevent distortion effects from the fluid meniscus. A calibrated Dino-Lite camera was positioned over top of the channel to capture images of channel dilation during step changes in head pressure (D: channel diameter; t: wall thickness). **(B):** Average channel diameter and Young's modulus as a function of relative pressure over the range of 0-150 Pa. Young's modulus was calculated via best fit ($R^2 > 0.99$) of a stress-strain model for cylindrical pressure vessels with variable modulus and thickness to experimental data. The error bars represent standard deviation (n = 6).

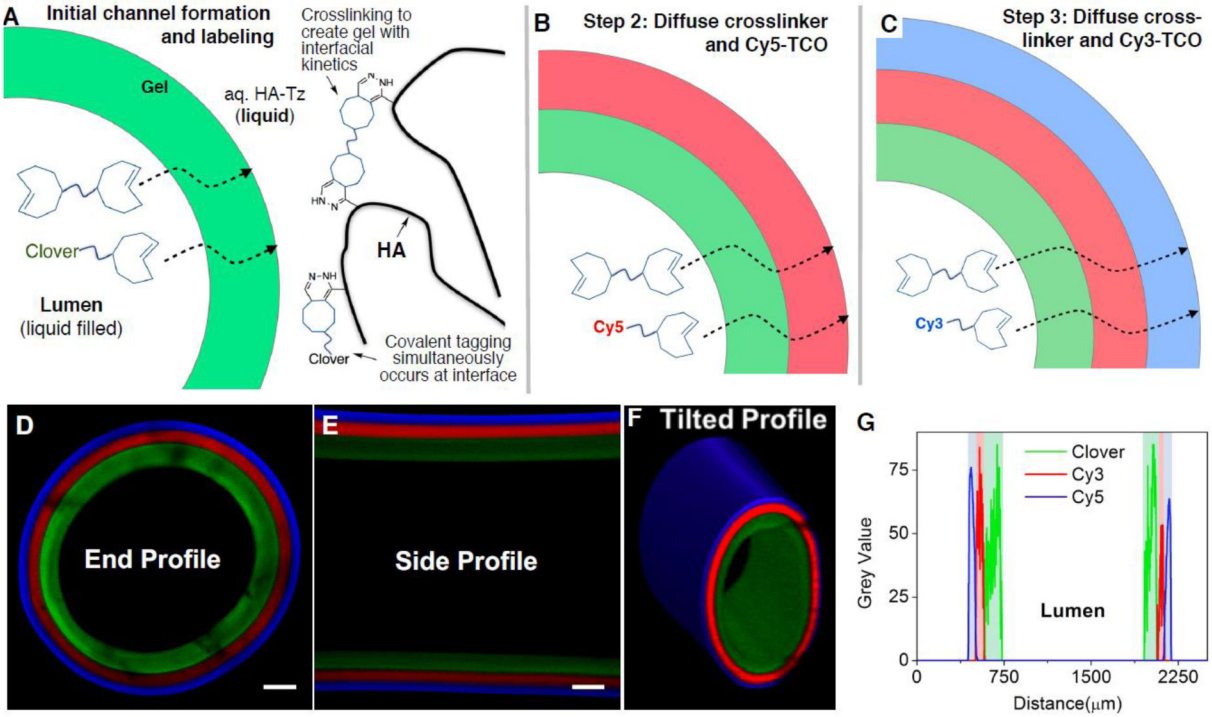

Figure 3.

Covalent patterning of TCO conjugated fluorophores in the channel wall. **(A-C):** Temporal supplementation TCO-conjugated fluorescent dye in the bisTCO crosslinker solution resulted in the spatial localization of the dye in the channel wall. A bisTCO solution containing 4.4 mM PEG-bisTCO and 5 μM TCO-conjugated Clover (green), Cy5 (red) or Cy3 (blue) was used. The crosslinking reaction was allowed to proceed for 5 **(A),** 15 **(B)** and 45 **(C)** min, respectively. **(D-F):** Confocal imaging confirmed covalent tagging and spatial localization of the fluorescence dyes. Scale bar = 200 μm. **(G):** Intensity plot across the channel wall showing the thickness of each layer.

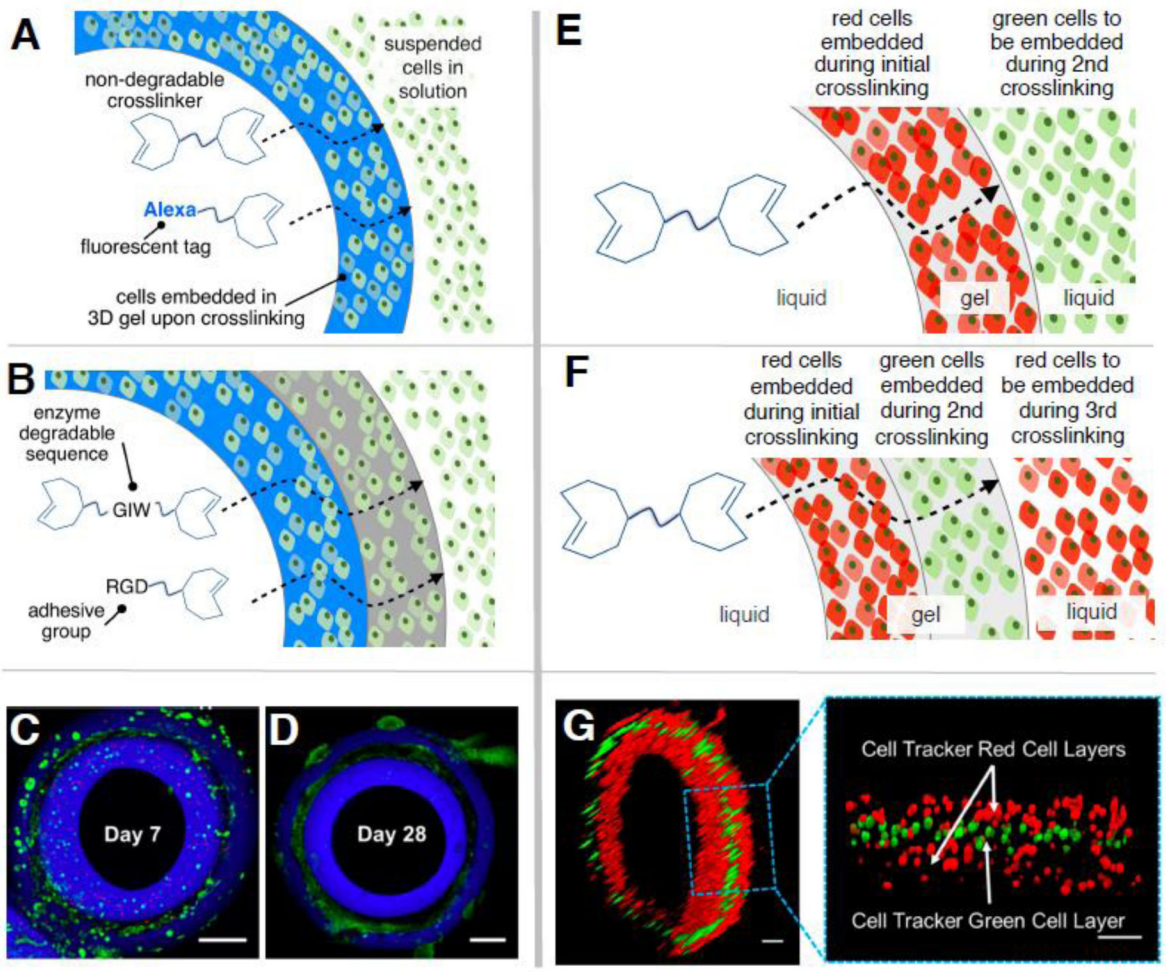

Figure 4.

Spatial patterning of peptides and cells in crosslinked hydrogel channels. **(A-D):** Trilaminate hydrogel channels were produced *via* temporal alteration of TCO solution composition. The inner and the outer layers (blue) were formed using PEG-bisTCO (5 mM) and Alexa-TCO (2 μM) while the middle region (black) was established using GIW-bisTCO (3.2 mM and RGD-TCO (0.4 mM). NIH3T3 fibroblasts were dispersed in HA-Tz and encapsulated in the channel wall homogeneously **(A, B).** Confocal images show fibroblast-populated hydrogels after 7 **(C)** and 28 **(D)** days of culture. Fibroblasts were transfected with green fluorescent protein and dead cells were stained red by ethidium homodimer. Scale bar = 200 μm. **(E-G):** NIH3T3 fibroblasts stained with Cell Tracker Red or Cell Tracker Green were patterned into the hydrogel channel via sequential alteration of the cell population in the HA-Tz bath **(E, F).** Confocal z-stack images **(G)** confirmed the trilaminate structure with alternating red-green-red cells. Scale bar =100 μm.

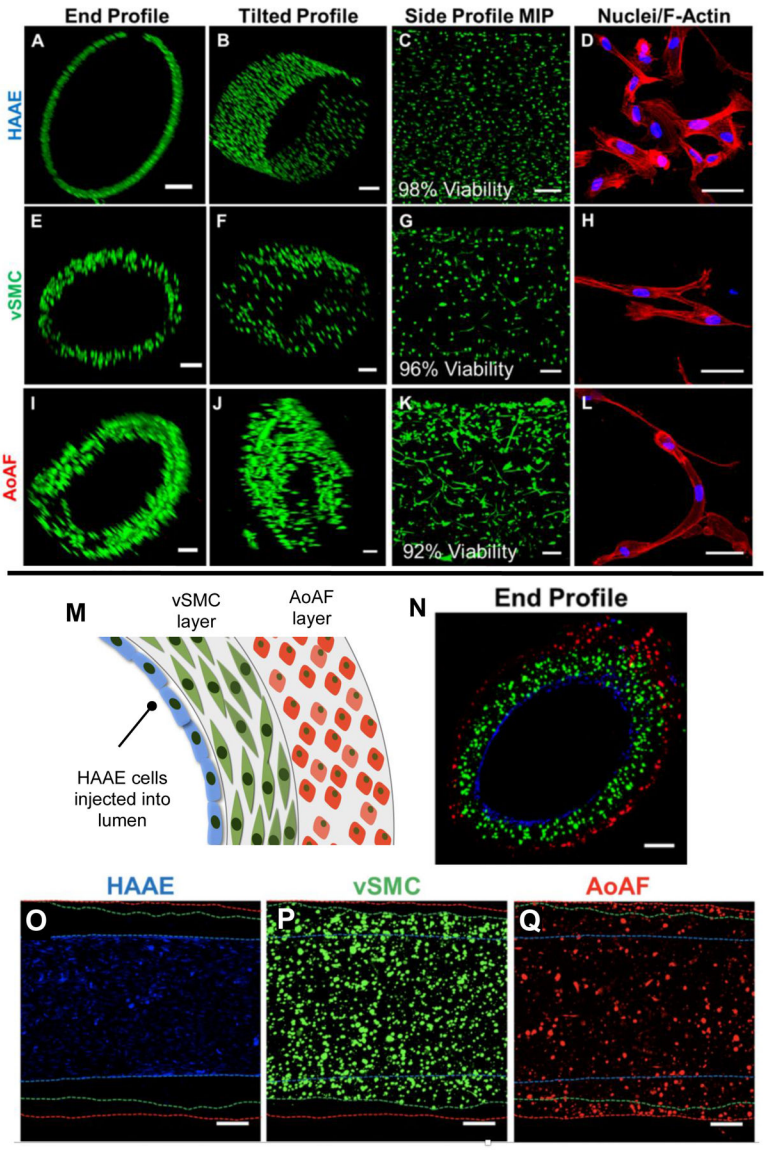

Figure 5.

Encapsulation and patterning of vascular cells found in the native blood vessel. **(A-L):** Encapsulation and culture of a single cell type. Vascular endothelial (HAAE, **A-D**) were cultured on the inner wall, smooth muscle cells (vSMC, **E-H**) and fibroblasts (AoAF, **I-L**) were 3D encapsulated in the channel wall. Cells were cultured for 7 days and were stained with calcein AM (green) and ethidium homodimer (red) for viability analysis (**A-C, E-G, I-K**, Scale bar = 200 μm). For morphological analysis (**D, H, L**, Scale bar = 50 μm), constructs were fixed and stained with DAPI (blue) and phalloidin (red). **(M-Q):** 3D patterning of endothelial cells, smooth muscle cells and fibroblasts. The three cell types were stained with cell trackers and patterned into the channel, with the endothelial cells (blue) attached to the inner wall, the smooth muscle cells (green) in the first layer of the wall and the fibroblasts (red) in the outer layer of the wall. Confocal images (**N-Q**, scale bar =

200 μm) confirmed the spatial localization of the three cell types in the correct anatomical order.